Cerebral Cortex, July 2017;27: 3618–3629

doi: 10.1093/cercor/bhw183
Advance Access Publication Date: 29 August 2016
Original Article

ORIGINAL ARTICLE

Palmitoylation of cdc42 Promotes Spine Stabilization and Rescues Spine Density Deficit in a Mouse Model of 22q11.2 Deletion Syndrome

E. Moutin[1], I. Nikonenko[1], T. Stefanelli[1], A. Wirth[2], E. Ponimaskin[2], M. De Roo[1], and D. Muller[1,†]

[1]Department of Basic Neurosciences, Medical School, University of Geneva, 1211 Geneva 4, Switzerland and [2]Cellular Neurophysiology, Hannover Medical School, 30625 Hannover, Germany

Address correspondence to Enora Moutin, Institut de Génomique fonctionnelle, 141 rue de la cardonille, 34094 Montpellier, France. Email: enora.moutin@igf.cnrs.fr; Mathias De Roo, Department of Basic Neurosciences, Medical School, University of Geneva, 1211 Geneva 4, Switzerland. Email: Mathias.DeRoo@unige.ch
[†]Deceased

Abstract

22q11.2 deletion syndrome (22q11DS) is associated with learning and cognitive dysfunctions and a high risk of developing schizophrenia. It has become increasingly clear that dendritic spine plasticity is tightly linked to cognition. Thus, understanding how genes involved in cognitive disorders affect synaptic networks is a major challenge of modern biology. Several studies have pointed to a spine density deficit in 22q11DS transgenic mice models. Using the LgDel mouse model, we first quantified spine deficit at different stages using electron microscopy. Next we performed repetitive confocal imaging over several days on hippocampal organotypic cultures of LgDel mice. We show no imbalanced ratio between daily spine formation and spine elimination, but a decreased spine life expectancy. We corrected this impaired spine stabilization process by overexpressing ZDHHC8 palmitoyltransferase, whose gene belongs to the LgDel microdeletion. Overexpression of one of its substrates, the cdc42 brain-specific variant, under a constitutively active form (cdc42-palm-CA) led to the same result. Finally, we could rescue spine density in vivo, in adult LgDel mice, by injecting pups with a vector expressing cdc42-palm-CA. This study reveals a new role of ZDHHC8-cdc42-palm molecular pathway in postsynaptic structural plasticity and provides new evidence in favor of the dysconnectivity hypothesis for schizophrenia.

Key words: confocal imaging, dendritic spine, DiGeorge syndrome, hippocampus, plasticity

Introduction

22q11DS (or velocardiofacial syndrome, or DiGeorge syndrome) is an autosomal dominant pathology caused by a de novo deletion of 1.5–3 MB of the HSA22q11 region on the human chromosome 22 (Carlson et al. 1997). Patients suffering from this syndrome present an array of physiological and behavioral deficits (Shprintzen et al. 1978; Goldberg et al. 1993; Paylor et al. 2001; Long et al. 2006) and about 30% of them will develop schizophrenia or shizoaffective behavior (Pulver et al. 1994). This makes 22q11DS the highest known genetic risk factor for developing schizophrenia. Considerable work has been done over the last 20 years to address the complex etiology of this pathology. The hemizygous deletion of the human chromosomal region 22q11.2 contains 28 functional genes, all but one being present in the orthologous region of mouse chromosome 16, allowing the generation of mice models (Merscher et al. 2001; Stark et al. 2008). Behavioral tests have been performed on these mice with the aim of linking cognitive deficits with

specific brain dysfunction (Long et al. 2006; Arguello and Gogos 2010; Karayiorgou et al. 2010; Meechan et al. 2015).

One of the key determinants for the establishment of neuronal networks is the formation of excitatory synaptic contacts on dendritic spines. A fine-tuning of spine formation versus elimination is driven throughout life by synaptic plasticity (Engert and Bonhoeffer 1999; De Roo et al. 2008b) that occurs upon sensory experience and learning (Bhatt et al. 2009; Holtmaat and Svoboda 2009; Kasai et al. 2010; Caroni et al. 2012). Understanding the rules underlying spine dynamics is thus essential to figure out how brain develops synaptic networks capable of accurate information processing.

Among deleted genes in 22q11DS, *zdhhc8* is part of a family of 23 palmitoyltransferase (PAT) enzymes which catalyze palmitoylation of target proteins. Palmitoylation is the covalent attachment of palmitic acid, especially to cysteines of the proteins, through a thioester bond, which confers to this posttranslational modification a reversible nature. Because palmitoylation is a dynamic process, it is involved in the regulation of many molecular mechanisms including protein localization, stability and trafficking (Salaun et al. 2010). The cycles between palmitoylated and depalmitoylated states are constitutive or dynamically regulated by extracellular signals. Among the ZDHHC8 targets, there are some important synaptic proteins, such as postsynaptic density protein 95 (PSD-95), palmitoylation of which is involved in the regulation of synaptic strength (El-Husseini et al. 2002). It raised the hypothesis that impairment in palmitoylation could lead to cognitive dysfunction and pathology (Fukata and Fukata 2010). More recently, a neural palmitoyl-proteomics characterized a brain-specific cdc42 splice variant as a palmitoylated substrate, cdc42-palm, in addition to the cdc42-prenyl splice variant which is ubiquitously expressed (Kang et al. 2008). Cdc42 is part of the Rho family of small GTPases and is involved in structural and synaptic plasticity (Rex et al. 2009; Vadodaria et al. 2013). Interestingly, the brain-specific variant cdc42-palm is enriched in dendritic spines and its localization depends on its palmitoylated state, which is tightly regulated by synaptic activity (Kang et al. 2008).

A recent publication showed presynaptic impairments in a 22q11DS mouse model such as impaired axonal growth, attributed at least in part to a decreased palmitoylation of cdc42 (Mukai et al. 2015). From the postsynaptic point of view, it was shown earlier that dendritic complexity and spine density are altered in these mice (Mukai et al. 2008; Fenelon et al. 2013). Also, this was attributed in part to the lack of ZDHHC8, this time supposedly through the lack of palmitoylation of PSD-95 (Mukai et al. 2008). Although spine density deficit has been further confirmed in a mouse model of 22q11DS (Xu et al. 2013), its developmental aspects have only been studied in neurons from dissociated cultures (Mukai et al. 2008), letting space for compensation mechanisms specific to this model. Two-day spine turnover has been shown to be increased in vivo in these mice (Fenelon et al. 2013), but with unchanged formation versus elimination ratio, leaving open questions about the mechanisms of spine deficit.

In this study, we shed new light on several aspects of 22q11DS neuronal phenotype such as changes in spine density, spine dynamics and the role of ZDHHC8 and cdc42 in these alterations. For the first time, we characterized spine density deficit in LgDel mice, which carry a deletion equivalent to the typical 1.5 Mb 22q11.2 human deletion, at different developmental stages using ex vivo electron microscopy (EM). By following individual spines over days in hippocampal organotypic cultures, we then showed that the persistence of this low spine density is neither due to a deficit in spine formation nor to an unbalanced ratio between spine elimination and formation, but is indeed a consequence of an impaired long-term stabilization of spines. Next, we tested the role of ZDHHC8 in these mechanisms using overexpression and knockdown approaches, in wild type (WT) mice. Also, we demonstrated that spine stability deficit observed in LgDel mice can be corrected by overexpressing ZDHHC8. Exploring the substrates of ZDHHC8 that could be candidates for regulators of spine formation and elimination, we unraveled a role for cdc42-palm in long-term spine stabilization and showed that an overexpression of a constitutively active form of cdc42-palm is sufficient to set back spine stabilization to normal levels in LgDel mice. Finally, we successfully used this strategy to rescue in vivo spine density deficit in LgDel young adult mice.

Material and Methods

Animal Handling

All experiments were performed using a protocol approved by the Geneva veterinary office. All study was performed using the LgDel/+ mouse model (LgDel) generated by Prof. Raju Kucherlapati (Harvard) and WT littermates. This transgenic mouse model, similarly to the Df(16)A/- mouse, carries a deletion equivalent to the typical 1.5 Mb 22q11.2 human deletion.

Slice Cultures

Hippocampal organotypic slice cultures from postnatal 5–6 day LgDel mice or WT littermates were prepared with a 400 µm thickness, as previously described (Stoppini et al. 1991). Slices were cultured on a membrane confetti (Millipore, Schaffhausen, Switzerland) placed on an insert (Millipore, Schaffhausen, Switzerland) and maintained in a CO_2 incubator at 37 °C until DIV4 and then at 33 °C.

Plasmids, sh-RNAs and Adeno Associated Viruses

pCX-*mRFP1* and pcDNA3.1-*eGFP* were described previously (De Roo et al. 2008b). pcDNA3.1(+)-e*GFP-cdc42-palm*-CA was obtained by subcloning e*GFP* and *cdc42-palm* into pcDNA3.1(+) vector (Invitrogen, Zug, Switzerland) and mutation was introduced by using site-directed mutagenesis. The constitutively active (CA) cdc42 mutant used was the GTP-hydrolysis deficient G12V mutant. From pcDNA3.1(+)-e*GFP-cdc42-palm*-CA, we obtained pcDNA3.1(+)-e*GFP-cdc42-palm-mut*-CA by using site-directed mutagenesis to introduce a double-cysteine mutation (C188/189A). Adeno associated virus (AAV)-Syn-*eGFP-cdc42-palm-CA* was created by adding *cdc42-palm-CA* behind the synapsin promoter-driven *eGFP* of pAAV-Syn(0.5)-*eGFP*. *ZDHHC8* and *ZDHHC8-C134A* coding sequences were synthetized by genecust company (GENECUST EUROPE, Dudelange, Luxembourg) and subcloned into p-*Venus-DLC2* (Moutin et al. 2012) to obtain p-*Venus-ZDHHC8* and p-*Venus-ZDHHC8-C134A*. Sh-scramble-*RFP* and sh-*ZDHHC8-RFP* were both purchased from Origene company (provided by Labforce, Nunningen, Switzerland) and subcloned in pRFP-C-RS vector. The targeted sequence in *ZDHHC8* was CATGACCTTACAGCCACTGCGCTCTGAAG.

Slice Transfection and Imaging

Hippocampal organotypic slices from LgDel mice or WT littermates were transfected at day in vitro 7 (DIV7) with a biolistic method (Helios Gene Gun, Bio-Rad, Vaud, Switzerland) using

gold beads coated with appropriate plasmids. Confocal repetitive imaging and analysis was performed as previously published (De Roo et al. 2008b). Briefly, a secondary dendritic segment of ~30–40 µm length in the apical dendritic tree of a CA1 transfected neuron was imaged from DIV12 to DIV15 (at 0, 5, 24, 48, and 72 h) using an Olympus Fluoview 300 system. At least 3 independent batches of cultures were used for each condition. Only a single dendrite per organotypic slice was followed. 7–16 dendrites per condition were analyzed, resulting in 400–600 spines followed over time for each condition. Analysis was done by scrolling across each z-stack of images using a homemade plug-in developed for Osirix software (http://www.osirix-viewer.com), which allows manual identification and following of individual spine over time. Spine density was quantified at DIV15, which corresponds to the 72 h time point.

Pooled data from each condition are plotted as mean ± SEM and statistical significance was determined by *t*-test, one-way *ANOVA* or two-way *ANOVA*, as specified in the figure legends.

Electron Microscopy

The brains of LgDel mice and their WT littermates at different postnatal ages (P15, P24 and P41) were perfusion fixed, vibratome cut on 150 µm thick slices and embedded in EPON resin. Ultrathin serial sections (60 nm thick) were cut from the hippocampal CA1 area stratum radiatum and collected on single-slot Formvar-coated grids according to standard procedures. Serial images of the neuropil samples from the middle portion of CA1 stratum radiatum were taken using a transmission electron microscope Tecnai G212 (FEI Company, Oregon, United States of America) equipped with digital camera (Mega View III; Soft Imaging Systems), at a magnification of ×9700 (Tecnai G212).

For developmental analysis, spine synapse density was quantified on the aligned consecutive serial electron micrographs, in randomly selected volume samples of CA1 stratum radiatum, in the fields devoid of big processes and cell bodies, using the physical disector method (Sterio 1984). A total of 12 neuropil fields (238 disectors) from 2 P15 WT mice; 8 fields (130 disectors) from 2 P15 LgDel mice; 14 fields (220 disectors) from 2 P24 WT mice; 11 fields (168 disectors) from 2 P24 LgDel mice; 13 fields (244 disectors) from 2 P41 WT mice and 12 fields (176 disectors) from 2 P41 LgDel mice were analyzed.

For correlative confocal and EM, the brains of P41 LgDel mice unilaterally injected at P7 in the CA1 area of the hippocampus with AAV-Syn-eGFP-cdc42-palm-CA were perfusion fixed, processed for eGFP immunoperoxidase EM labeling as described (Nikonenko et al. 2008) and embedded in EPON resin. The pyramids were trimmed in the hippocampal CA1 stratum radiatum of the injected hemispheres and serial ultrathin (60 nm) sections were cut. Serial images of the labeled secondary apical dendrites of CA1 pyramidal neurons from 2 LgDel mice injected with the AAV construct were taken at magnification ×9700 (Tecnai G212). After alignment of the digital serial electron micrographs with Photoshop software (Adobe), 3D reconstructions were carried out using Neurolucida software (v6.02; MicroBrightField). In total, 10 dendritic segments from 2 AAV injected mice (total length: 91 µm) were reconstructed and spine synapse density, per unit length, was calculated. For comparison, dendritic segments from the secondary apical dendrites of CA1 pyramidal neurons in 2 control WT mice (P41; 9 dendritic segments, total length: 67.4 µm) and 2 control LgDel mice (P41; 9 dendritic segments, total length: 71.2 µm) were 3D reconstructed and spine synapse densities per unit length quantified. Pooled data from each condition are plotted as mean ± SEM and statistical significance was determined by one-way *ANOVA* or two-way *ANOVA*, as specified in the figure legends.

S-acylated Proteins Detection by Resin-assisted Capture (Acyl-rac)

Hippocampi from LgDel mice or WT littermates were mechanically dissociated in lysis buffer containing 25 mM Hepes, 25 mM NaCl, 1 mM EDTA, 0.5% triton and protease inhibitors (Roche, Basel, Switzerland). In order to block free SH groups, resuspended proteins were incubated with a blocking buffer containing 100 mM Hepes, 1 mM EDTA, 2.5% SDS, and 1.3% MMTS (S-methyl methanosulfonate, Sigma-Aldrich, Buchs St Gall, Switzerland) and incubated for 4 h at 40 °C with gentle agitation. Then, proteins were precipitated using cold 100% acetone and incubated for 20 min at −20 °C. After centrifugation, the pellet was air dried and washed 5 times by resuspending in 70% acetone. Pellets were resuspended in binding buffer containing 100 mM Hepes, 1 mM EDTA, 1% SDS and assessed to protein quantification using Pierce BCA assay (Thermo Instruments, Vaud, Switzerland). Twenty microgram per condition were kept for total extract at −20 °C, while the rest (1.3–1.5 mg) was splited in 2 parts and incubated with Thiopropyl Sepharose beads (Sigma-Aldrich, Buchs St Gall, Switzerland) that bind to free SH groups. In one part, hydroxylamine (NH2OH; Sigma-Aldrich, Buchs St Gall, Switzerland) at pH7.5 (cleaves off palmitate, resulting in free SH groups if proteins were palmitoylated) was added for a final concentration of 0.5 M, while in the other part, as a control, Tris pH7.5 was added with the same final concentration. After one night with agitation, beads were washed 5 times and proteins eluted in Laemmli buffer containing 50 mM DTT. Proteins were then resolved by SDS–PAGE, transferred onto nitrocellulose membranes, and detected by immunoblot using the following primary antibodies: PSD-95 (rabbit; Cell Signalling, provided by Millipore, Schaffhausen, Switzerland) and cdc42 (mouse, BD transduction laboratories, Allschwill, Switzerland). Pooled data from each condition are plotted as mean ± SEM and statistical significance was determined by *t*-test (Forrester et al. 2011).

Stereotaxical Surgery and AAV Injections

Anesthesia of P7 pups was induced at 5% and maintained at 1.5–2% isoflurane (w/v) (Baxter AG). Pups were placed in a stereotaxic frame (Angle One) and craniotomies were performed using stereotaxic coordinates adapted from a mouse brain atlas to target the dorsal CA1 of hippocampus: −1.40 anterior–posterior; ± 1.35 medial–lateral; −1.40 dorsal–ventral (from Lamda). For unilateral injections of AAV-Syn-eGFP-cdc42-palm-CA (150–300 nl per injection), we used graduated pipettes (Drummond Scientific Company, provided by Milian company, Geneva, Switzerland), broken back to a tip diameter of 10–15 µm, at an infusion rate of 0.05 µl/min. Micropipettes were left in place an additional 5 min following microinjection and slowly retracted (0.4 mm/min) to avoid reflux of the viral solution. At P37, some of these mice were anesthetized and fixed by intracardial perfusion with 4% paraformaldehyde to evaluate the efficiency of the viral infection. Brains were kept in 4% paraformaldehyde during 24 h, washed and then subjected to coronal sections of 60 µm thickness using a vibratome. Sections were processed for immunofluorescence to enhance eGFP signal. Briefly, slices were blocked and permeabilized in PBS

containing NGS 5% and triton 1%, incubated overnight with an antibody against eGFP (rabbit, Millipore, Schaffhausen, Switzerland) diluted in PBS containing NGS 5% and triton 0.5% and then incubated with appropriate secondary antibody. Images were acquired using an Olympus Fluoview 300 system. EM was performed 34 days after injections, at P41 on the other mice.

Results

Spine Density Deficit in LgDel Mice Revealed at Different Developmental Stages by ex vivo EM

We performed EM in CA1 area of LgDel and WT littermates hippocampi at 3 different developmental stages and quantified spine synapse density, per neuropil volume, on serial sections from neuropil volume samples. Spine density differences are illustrated on 3D reconstructed dendritic segments of WT and LgDel mice at P24 (Fig. 1A), and on representative EM images of the CA1 neuropil at P41 (Fig. 1B). As shown in Figure 1C, we observed a significant decrease in spine density in the infant LgDel mice entering the critical period of developmental synaptogenesis, after eye opening (P15; 1.95 ± 0.04 spines/μm^3 of neuropil volume, WT vs. 1.42 ± 0.08, LgDel, $P < 0.0001$), as well as in juvenile (P24; 2.63 ± 0.09, WT vs. 2.19 ± 0.04, LgDel, $P < 0.0001$) and young adult mice (P41; 2.72 ± 0.04, WT vs. 2.19 ± 0.05, LgDel, $P < 0.0001$), compared with WT littermates. We previously published that spine synapse density in WT mice increases between P15 and P24 to then remain stable (Nikonenko et al. 2013). Here, we confirmed these changes ($P < 0.0001$) and showed that LgDel mice follow the same developmental change ($P < 0.0001$) even though their spine density always remains at a lower level than in their WT littermates (−26.2% at P15, −17.6% at P24, and −19.3% at P41).

Long-term Preexisting Spine Stabilization Deficit in LgDel Mice Revealed by Repetitive Confocal Imaging

Several parameters of spine dynamics can influence spine density. A decreased spine density may, for example, be due to a defect of spine formation and/or increased spine elimination. In order to study spine dynamics in LgDel mice, we biolistically transfected hippocampal organotypic cultures from these mice and WT littermates with mRFP, at DIV7. We then performed repetitive confocal imaging on these slices from DIV12 to DIV15. In this model system, the hippocampal subnetwork is preserved and continues to develop for weeks (De Roo et al. 2008a). We followed individual spines of a secondary apical dendritic segment from a CA1 neuron over 4 days for both groups (Fig. 2A,B for representative images at 0 and 24 h for WT and LgDel, respectively). First, we confirmed our EM observations of a decreased spine density in LgDel mice compared with WT littermates (1.23 ± 0.08 in WT to 0.94 ± 0.09 in LgDel spines/μm of dendrite; −23.6% in LgDel; $P < 0.05$; Fig. 2C). Next, we quantified spine formation (Fig. 2D) as the percentage of new spines compared with previous observation and showed that spine formation in LgDel mice averaged on a 24-h period is significantly higher than in their WT littermates (19.2 ± 1.5% and 12.7 ± 1.3%, respectively; $P < 0.01$). This indicates that the spine density deficit in LgDel mice is not due to an abnormal low spine formation rate. The same analysis but for spine loss (Fig. 2E) revealed an increased spine elimination in LgDel mice (21.1 ± 1.9%, LgDel vs. 15.3 ± 1.5%, WT; $P < 0.05$). Overall, spine loss rate over 24 h is compensated by the rate of spine formation in WT and in LgDel mice and cannot explain by itself the spine density deficit observed in LgDel mice (Fig. 2F). Another parameter that can influence spine density is the long-term stabilization of the preexisting spine network. To explore this possibility, we considered all spines present at the first time

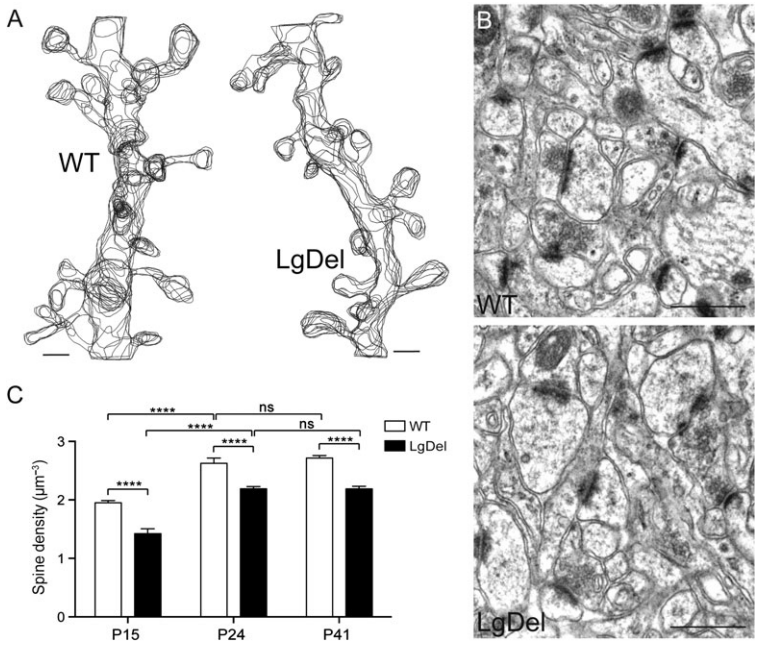

Figure 1. Spine synapse density in LgDel mice is lower than in WT mice throughout postnatal development. (*A*) 3D reconstructed dendritic segments of WT ($n = 19$ spines) and LgDel ($n = 15$ spines) mice at P24. Scale bars: 0.5 μm. (*B*) Representative EM images of the CA1 neuropil in WT (top) and LgDel (bottom) mice at P41. Scale bars: 0.5 μm. (*C*) Spine synapse density per μm^3 of neuropil volume in WT and LgDel mice at different time points of postnatal development, quantified with EM. Data show the averages ± SEM of spine synapse densities from at least 10 disectors per 8–14 places analyzed. ****$P < 0.0001$. ns: not significant; two-way ANOVA. Further details on the EM analysis in the Material and Methods section.

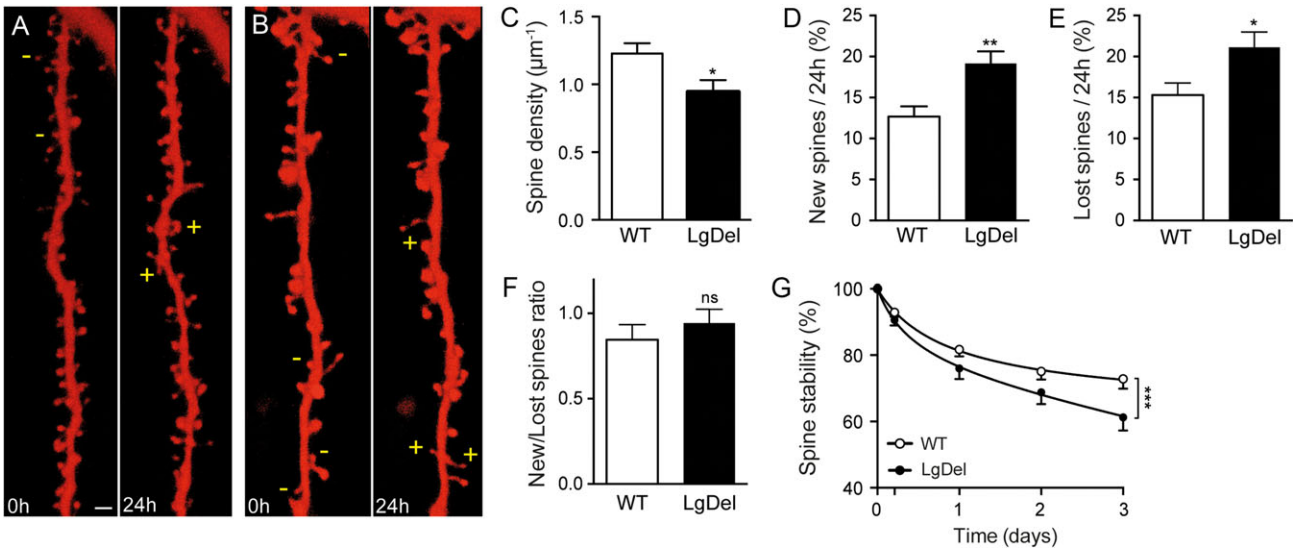

Figure 2. Long-term spine stability is decreased in LgDel mice compared with WT mice. (*A, B*) Representative images at 0 and 24 h of mRFP transfected WT (A) or LgDel (B) dendritic segments (30–40 µm length) from pyramidal CA1 neurons. Plus and minus signs indicate spine appearance and disappearance between the 2 time points, respectively. Scale bar: 1 µm. (*C*) Spine density per µm of dendritic segments transfected with mRFP in WT (white bar) and LgDel (black bar). (*D*) Percentage of spine formation per 24 h periods for WT (white bar) and LgDel (black bar). (*E*) Same as D, but for spine loss. (*F*) Ratio of the percentages of newly over lost spines per 24 h periods in WT (white bar) and LgDel (black bar). (*G*) Preexisting spine stability as a function of time for WT (white circles) and LgDel (black circles). Each circle represents the average percentage of spines present at 0 h that are still present at subsequent observations. ***$P < 0.001$; two-way ANOVA. In *C*, *D*, *E*, and *F*, data show the mean ± SEM of 10 (LgDel) to 11 (WT) dendrites, one dendrite per animal. *$P < 0.05$. **$P < 0.01$. ns: not significant; unpaired *t*-test.

point and followed them individually during 3 more days. This analysis unraveled a significant impairment of preexisting spine stabilization over 4 days in LgDel mice versus WT littermates ($P < 0.001$, Fig. 2*G*) with an average of 61% of 4-day stable spines in LgDel compared with 73% in WT littermates.

Together, these results indicate that the spine density deficit observed in ex vivo EM study of LgDel mice is faithfully reproduced in hippocampal organotypic culture, and point on an impaired long-term spine stabilization process in LgDel mice.

Genetic Rescue of ZDHHC8 PAT Activity Restores Long-term Spine Stabilization in Hippocampal Slices from LgDel Mice

Among the array of genes deleted in 22q11DS patients, *ZDHHC8* is of particular interest because palmitoylation is involved in synaptic function (El-Husseini et al. 2002; Lin et al. 2009; Fukata and Fukata 2010; Milnerwood et al. 2013; Thomas et al. 2013). Moreover, overexpression of ZDHHC8 has been shown to nearly compensate spine density deficits in dissociated cultures of a mouse model of 22q11DS (Mukai et al. 2008). In order to better understand the consequences of ZDHHC8 enzymatic activity, we first checked the level of ZDHHC8 mRNA in LgDel hippocampi and found that it was decreased by 50% compared with WT (Supplementary Fig. 1), as expected considering the haploinsufficiency. This diminution in ZDHHC8 mRNAs level was specific, since the mRNAs levels of other structurally and/or functionally related PATs (Fukata and Fukata 2010) were not changed in LgDel mice hippocampi (Supplementary Fig. 1). Then we performed, as previously, repetitive confocal imaging on WT hippocampal organotypic slices either with overexpressed or downregulated ZDHHC8. The quantification of spine density at DIV15 is summarized in Figure 3*A* and representative images can be viewed in Supplementary Fig. 2. Overexpression of ZDHHC8 produced a significant increase in spine density (1.23 ± 0.08 spines/µm of dendrite, WT vs. 1.50 ± 0.08, WT + ZDHHC8; $P < 0.05$), while knockdown of ZDHHC8 by sh-RNA strategy (see Supplementary Fig. 3 for the sh-RNA efficiency) caused a significant decrease in spine density (1.23 ± 0.08 spines/µm of dendrite, WT vs. 0.70 ± 0.08, WT + sh-ZDHHC8; $P < 0.001$).

Analysis of spine stability over 4 days showed a slight but significant increase in spine stabilization as a consequence of ZDHHC8 overexpression ($P < 0.001$, Fig. 3*B*). Conversely, knockdown of ZDHHC8 expression led to a strong decrease in spine stabilization ($P < 0.0001$, Fig. 3*C*). Neither the transfection of a scramble sh-RNA nor the overexpression of the punctual mutant ZDHHC8-C134A that blocks the enzymatic activity significantly changed the spine density or stabilization, thus validating our sh-RNA strategy and confirming that the effect of ZDHHC8 on spine density was due to its enzymatic activity (Fig. 3*A*,*B*,*C*).

Based on these observations, we next overexpressed ZDHHC8 in hippocampal organotypic slices from LgDel mice and analyzed spine dynamics as mentioned above. Using this strategy, spine density was successfully rescued to WT levels (1.23 ± 0.08 spines/µm of dendrite, WT; 1.23 ± 0.08, LgDel + ZDHHC8; Fig. 3*D* and Supplementary Fig. 2 for representative images), confirming previous observations (Mukai et al. 2008). Interestingly, overexpression of ZDHHC8 did not allow a scaling down of spine formation to control levels (12.7 ± 1.3%, WT; 19.2 ± 1.5%, LgDel; 20.8 ± 1.9%, LgDel + ZDHHC8; Fig. 3*E*), whereas it led to a decrease in spine loss close to WT rate (14.4 ± 1.4%, LgDel + ZDHHC8; 21.1 ± 1.9%, LgDel; 15.3 ± 1.5%, WT; Fig. 3*F*). We then monitored the stability of preexisting spines and showed that ZDHHC8 expression restores spine stability in LgDel neurons close to WT level (At 72 h, 61.3 ± 4.0% in LgDel, 72.9 ± 2.9% in WT, and 78.6 ± 2.3% in LgDel + ZDHHC8; Fig. 3*G*).

These series of experiments first strongly suggest that one or several substrates of ZDHHC8 are switchable molecular determinants of spine dynamics. Second, they provide

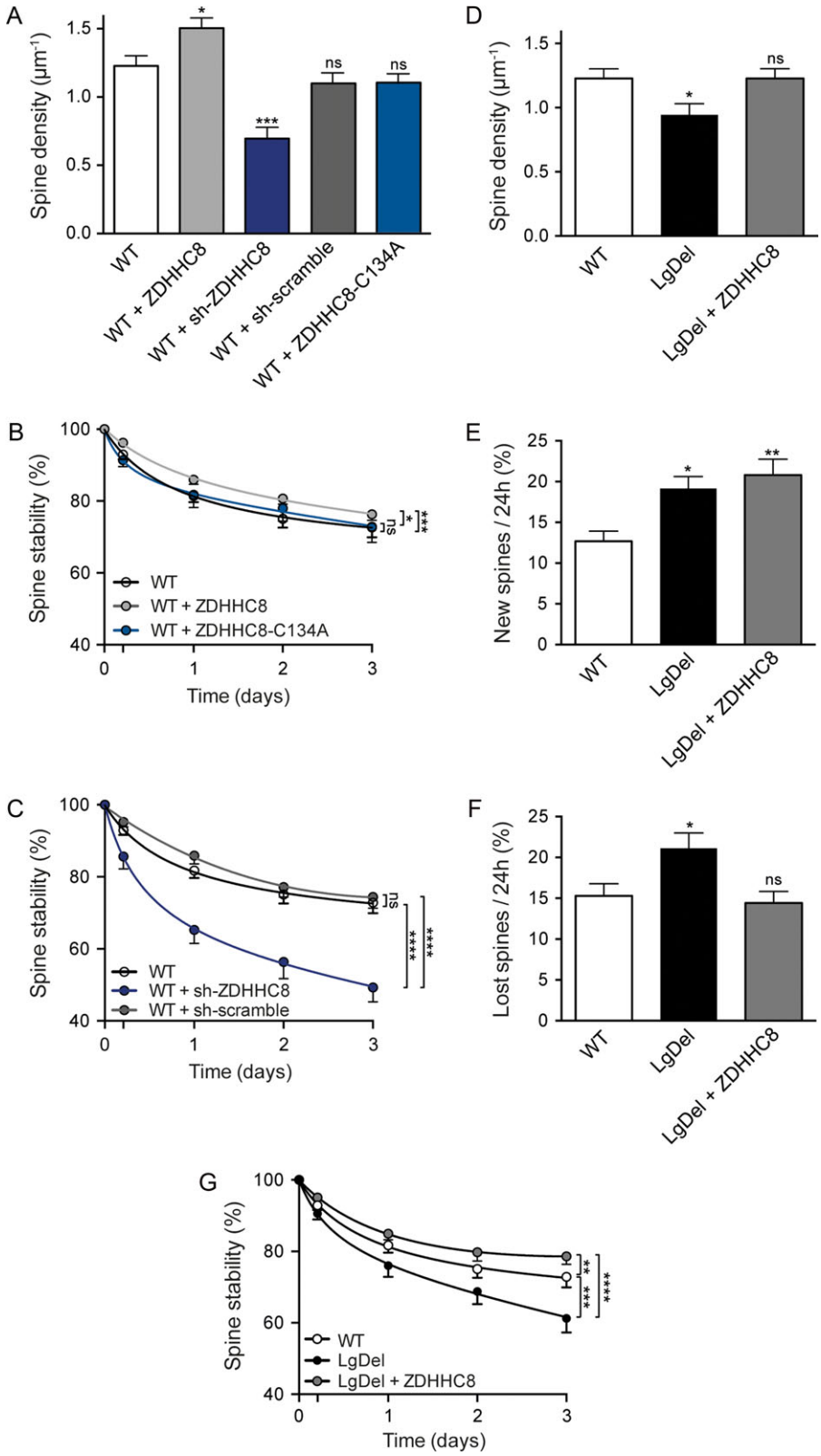

Figure 3. ZDHHC8 PAT activity restores spine stabilization in LgDel mice. (*A*) Spine density per µm of dendritic segments (30–40 µm length) of WT pyramidal CA1 neurons transfected with mRFP (white bar), mRFP + Venus-ZDHHC8 (light gray bar), eGFP + sh-ZDHHC8-RFP (dark blue bar), eGFP + sh-scramble-RFP (dark gray bar) or mRFP + Venus-ZDHHC8-C134A (blue bar). (*B*) Spine stability over time in WT pyramidal CA1 neurons transfected with mRFP (white circles, $n = 11$), mRFP + Venus-ZDHHC8 (gray circles, $n = 15$) or mRFP + Venus-ZDHHC8-C134A (blue circles, $n = 8$). (*C*) Same as *B* but with mRFP (white circles, $n = 11$), eGFP + sh-ZDHHC8-RFP (blue circles, $n = 8$), eGFP + sh-scramble-RFP (gray circles, $n = 8$). (*D*) Same as *A* but in WT (white bar) and LgDel (black bar) neurons transfected with mRFP and in LgDel neurons transfected with mRFP + Venus-ZDHHC8 (gray bar). (*E*) Percentage of spine formation per 24 h periods in WT (white bar) and LgDel (black bar) neurons transfected with mRFP and in LgDel neurons transfected with mRFP + Venus-ZDHHC8 (gray bar). (*F*) Same as *E*, but for spine disappearance. (*G*) Same as *B* but in WT

evidence that deficient spine density and long-term spine stability observed in hippocampal organotypic cultures of LgDel mice can be re-established by a genetic reintroduction of ZDHHC8.

Genetic Rescue of cdc42 palmitoylation Restores Long-term Spine Stabilization in Hippocampal Slices from LgDel Mice

Several synaptic proteins can be modulated by palmitoylation (Fukata and Fukata 2010). Among them, PSD-95 (previously shown as a target of ZDHHC8; Mukai et al., 2008) and cdc42 are both involved in many aspects of structural and synaptic plasticity (Meyer et al. 2014). Cdc42 exists in 2 splicing variants, cdc42-prenyl, which is ubiquitously expressed, and cdc42-palm, a brain-specific form that can be modulated by palmitoylation (Kang et al. 2008). We performed the acyl-rac method, which allows the pull-down of all palmitoylated proteins in hydroxylamine (NH_2OH) condition (Forrester et al. 2011) on fresh hippocampi from LgDel mice and WT littermates. A staining with an antibody against PSD-95 showed no significant change in PSD-95 palmitoylation (–9.9 ± 8.9% in LgDel vs. WT condition; Fig. 4A,B), while a staining of the same membranes with an antibody against cdc42 revealed a strong decrease of palmitoylated cdc42 in LgDel condition compared with WT (–77.9 ± 6.9%, $P < 0.0001$; Fig. 4A,B). It is noteworthy that neither changes in cdc42-palm mRNA expression (Supplementary Fig. 4A) nor in cdc42-palm expression at the protein level were detected (Fig. 4A, total extracts). Importantly, the 2 cdc42 variants, cdc42-palm and cdc42-prenyl, presented the same mRNA expression in WT and LgDel hippocampi (Supplementary Fig. 4A,B, respectively). These experiments show that the haploinsufficiency of *zdhhc8* induces a drastic reduction of the level of palmitoylated cdc42 in hippocampus.

Based on these results and our previous study where we demonstrated that cdc42-palm palmitoylation can modulate cellular morphology (Wirth et al. 2013), we then checked if cdc42-palm could rescue spine dynamic properties in LgDel mice by performing repetitive confocal imaging on LgDel hippocampal organotypic slices. Overexpression of a constitutively active form of cdc42-palm, cdc42-palm-CA, fully rescued spine density in LgDel neurons (0.94 ± 0.09 spines/µm of dendrite, LgDel vs. 1.23 ± 0.08, WT and 1.19 ± 0.05, LgDel + cdc42-palm-CA; Fig. 4C and Supplementary Fig. 2 for representative images). Regarding spine dynamics, new spine rate over 24 h was not fully set back to the WT level (12.7 ± 1.3, WT; 19.2 ± 1.5%, LgDel and 15.7 ± 2.2%, LgDel + cdc42-palm-CA; Fig. 4D), whereas spine loss was strongly decreased (15.3 ± 1.5%, WT; 21.1 ± 1.9%, LgDel and 12.0 ± 0.7%, LgDel + cdc42-palm-CA; Fig. 4E). Finally, long-term analysis showed a strong improvement of 4-day preexisting spine stability in LgDel mice after cdc42-palm-CA overexpression (Fig. 4F), resulting in a significantly higher spine survival at 4 days in LgDel mice overexpressing cdc42-palm-CA (61 ± 4%, LgDel vs. 77 ± 2%, LgDel + cdc42-palm-CA; $P < 0.0001$), and comparable to the LgDel + ZDHHC8 values (78.6 ± 2.3%). Importantly, expression of cdc42-palm-mut-CA, a double-cysteine mutant that abolishes palmitoylation, does not change density, turnover or stability of dendritic spines in LgDel slices (Supplementary Fig. 5).

All together, these experiments show that in a mouse model of 22q11DS, the haploinsufficiency of *zdhhc8* leads to a strong decrease in the level of the posttranslational palmitoylation of cdc42 in the hippocampus, and that cdc42-palm palmitoylation is necessary and sufficient to fully rescue spine density by restoring correct dendritic spine stability.

In vivo Injection of an AAV Carrying a Constitutively Active Form of cdc42-palm Rescues Spine Density in Adult LgDel Mice

Based on our previous results obtained in organotypic cultures, we aimed to determine if cdc42-palm expression could rescue spine density in LgDel mice in vivo. For this, we unilaterally injected P7 LgDel pups in the CA1 area of hippocampus with an AAV construct carrying the constitutively active form of cdc42-palm tagged with eGFP, the AAV-Syn-eGFP-cdc42-palm-CA. Importantly, we did not notice any physiological or behavioral disturbances in injected mice during their whole growth period from P7 to young adult stage. These mice were perfused at P41 and their brains were processed for the EM. CA1 pyramidal neurons infected with the AAV construct were clearly visible by confocal microscopy in the injected hemisphere (Fig. 5A). This staining was converted to the electron-dense diaminobenzidine precipitate using preembedding immunoperoxidase technique for further EM analysis (Fig. 5B). Labeled secondary apical dendritic segments of CA1 pyramidal neurons infected with the AAV-Syn-eGFP-cdc42-palm-CA construct were then 3D reconstructed in the stacks of serial electron micrographs and spine density per micrometer of dendrite length was calculated. In total, we reconstructed 10 dendritic segments from 2 AAV injected LgDel mice (total length: 91 µm) (Fig. 5C). For comparison, we quantified spine density per micrometer of dendrite length on 3D reconstructed dendritic segments from the secondary apical dendrites of CA1 pyramidal neurons in 2 control WT mice (P41; 9 dendritic segments, total length: 67.4 µm) and 2 control LgDel mice (P41; 9 dendritic segments, total length: 71.2 µm) (Fig. 5D,E, respectively). We have reported previously that eGFP expression in neurons does not change spine density (Nikonenko et al. 2008). Analysis of the 3D EM data has shown that injection with AAV-Syn-eGFP-cdc42-palm-CA fully rescued spine density in LgDel mice (3.82 ± 0.24 spines/µm of dendrite) compared with control WT (3.53 ± 0.14, ns) and LgDel mice (2.89 ± 0.08, $P < 0.01$) (Fig. 5F).

These experiments show that in vivo expression of a constitutively active form of cdc42-palm is sufficient to fully rescue spine density in LgDel mice.

Discussion

In this study, we elucidate the role of the palmitoylation enzyme ZDHHC8 in the regulation of spine density by identifying one of its substrates, cdc42-palm, as a key molecular determinant of long-term spine stabilization.

By overexpressing a constitutively active form of cdc42-palm and cdc42-palm-CA, we were able to set back normal long-term spine stabilization and recover normal spine density

(white circles, $n = 11$) and LgDel (black circles, $n = 10$) neurons transfected with mRFP and in LgDel neurons transfected with mRFP + Venus-ZDHHC8 (gray circles, $n = 16$). In A, D, E, and F, data are the mean ± SEM of 8 (WT + sh-ZDHHC8; WT + sh-scramble; WT + ZDHHC8-C134A), 10 (LgDel), 11 (WT), 15 (WT + ZDHHC8), 16 (LgDel + ZDHHC8) dendrites, one dendrite per animal. *$P < 0.05$. **$P < 0.01$. ***$P < 0.001$. ns: not significant; one-way ANOVA. In B, C, and G, each circle represents the average percentage of spines present at 0 h that are still present at subsequent observations. *$P < 0.05$. **$P < 0.01$. ***$P < 0.001$. ****$P < 0.0001$. ns: not significant; two-way ANOVA.

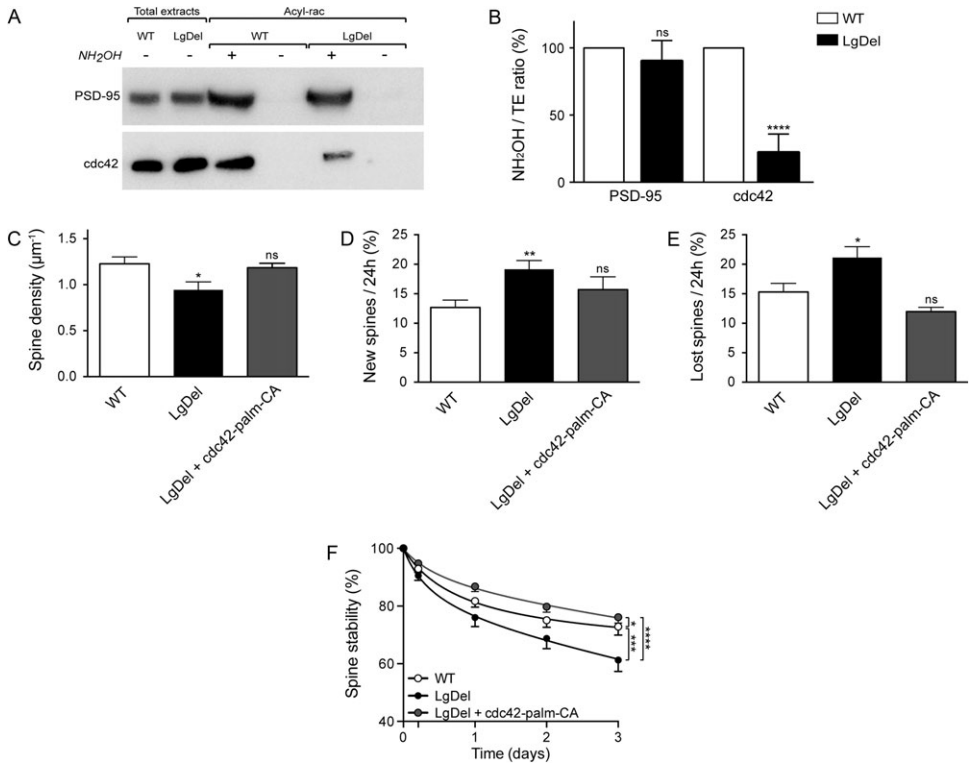

Figure 4. Cdc42 palmitoylation restores spine stabilization in LgDel mice. (*A*) Palmitoylation of PSD-95 and cdc42 in WT and LgDel hippocampi detected by the acyl-rac method and revealed by western blot. Note that there is no change in PSD-95 and cdc42 expression in the total extracts in WT compared with LgDel hippocampi. (*B*) Quantification of the percentage of palmitoylated cdc42 and PSD-95 normalized to their respective total extracts, in WT and LgDel hippocampi. Data are mean ± SEM of 3 independent experiments, each one being done with hippocampi from an LgDel mouse and a WT littermate. ****$P < 0.0001$. ns: not significant; *t*-test. (*C*) Spine density per µm of dendritic segments (30–40 µm length) in mRFP transfected WT (white bar) and LgDel (black bar) neurons and in LgDel neurons transfected with eGFP-cdc42-palm-CA + mRFP (gray bar). (*D*) Percentage of spine formation per 24 h periods in WT (white bar) and LgDel (black bar) neurons transfected with mRFP and in LgDel neurons transfected with mRFP + eGFP-cdc42-palm-CA (gray bar). (*E*) Same as *D*, but for spine disappearance. (*F*) Spine stability variation with time in WT (white circles, $n = 11$) and LgDel (black circles, $n = 10$) neurons transfected with mRFP and in LgDel neurons transfected with mRFP + eGFP-cdc42-palm-CA (gray circles, $n = 8$). Each circle represents the average percentage of spines present at 0 h that are still present at subsequent observations. *$P < 0.05$. ***$P < 0.001$. ****$P < 0.0001$; two-way *ANOVA*. In *C*, *D*, and *E*, data are the mean ± SEM of 8 (LgDel + cdc42-palm-CA), 10 (LgDel), 11 (WT) dendrites, one dendrite per animal. *$P < 0.05$. **$P < 0.01$. ns: not significant; one-way *ANOVA*.

in a genetic mouse model of 22q11DS (LgDel) where *zdhhc8* is haploinsufficient. Furthermore, we successfully rescued spine density in adult LgDel mice in vivo by injecting pups with a virus containing a cdc42-palm-CA construct.

The Spine Density Deficit in LgDel Mice

Spine density has been shown to be decreased in mice models of 22q11DS, but the extent of this decrease varied from 20% to 50% depending on the technique, area and developmental stage chosen (Mukai et al. 2008; Xu et al. 2013), and was not observed in all brain areas (Fenelon et al. 2013). In this study, we systematically quantified the spine density in LgDel mice and WT littermates hippocampus using ex vivo EM, at 3 key developmental stages: P15 (young animals), P24 (juvenile) and P41 (young adult) and showed that LgDel mice exhibit a systematic spine density deficit at these 3 stages while being able to increase their spine density following the postnatal developmental pattern of WT mice (Nikonenko et al. 2013). Spine density is believed to be regulated by genetic and environmental factors (Yoshihara et al. 2009). Together with other studies (Mukai et al. 2008, 2015; Fenelon et al. 2011), our results indicate that brains from a 22q11DS mouse model have impaired spine density early in development. Importantly, we also reveal that while keeping the capacity to create new spines, pyramidal neurons in hippocampus of infant, juvenile and adult LgDel mice are never able to produce a normal spine density.

The Spine Dynamics Behind the Spine Density Deficit in LgDel Mice

Both impaired spine formation and exaggerated spine elimination can result in a low spine density. In schizophrenia models, it has been suggested that an imbalance between these 2 parameters lies behind the spine density deficit (Kasai et al. 2010). It thus appeared evident to study spine dynamics in order to identify whether spine formation and/or spine elimination is altered. However, a recent two-time point in vivo 2-photon experiment on cortical neurons from a 22q11DS mouse model did not show such an imbalance. Instead, both spine formation and elimination were equally increased in these mice (Fenelon et al. 2013). This result may be explained by the fact that probability of spine elimination is different depending on spine age. Spine formed within a few hours has a very small life expectancy, while spine that remained stable for at least 1 day has a much longer one (De Roo et al. 2008a; Holtmaat et al. 2005). Based on this knowledge, we performed repetitive confocal imaging in hippocampal slice cultures over 4 days and identified a strong impairment of long-term stability of preexisting spines. Although this result does not exclude a defect in

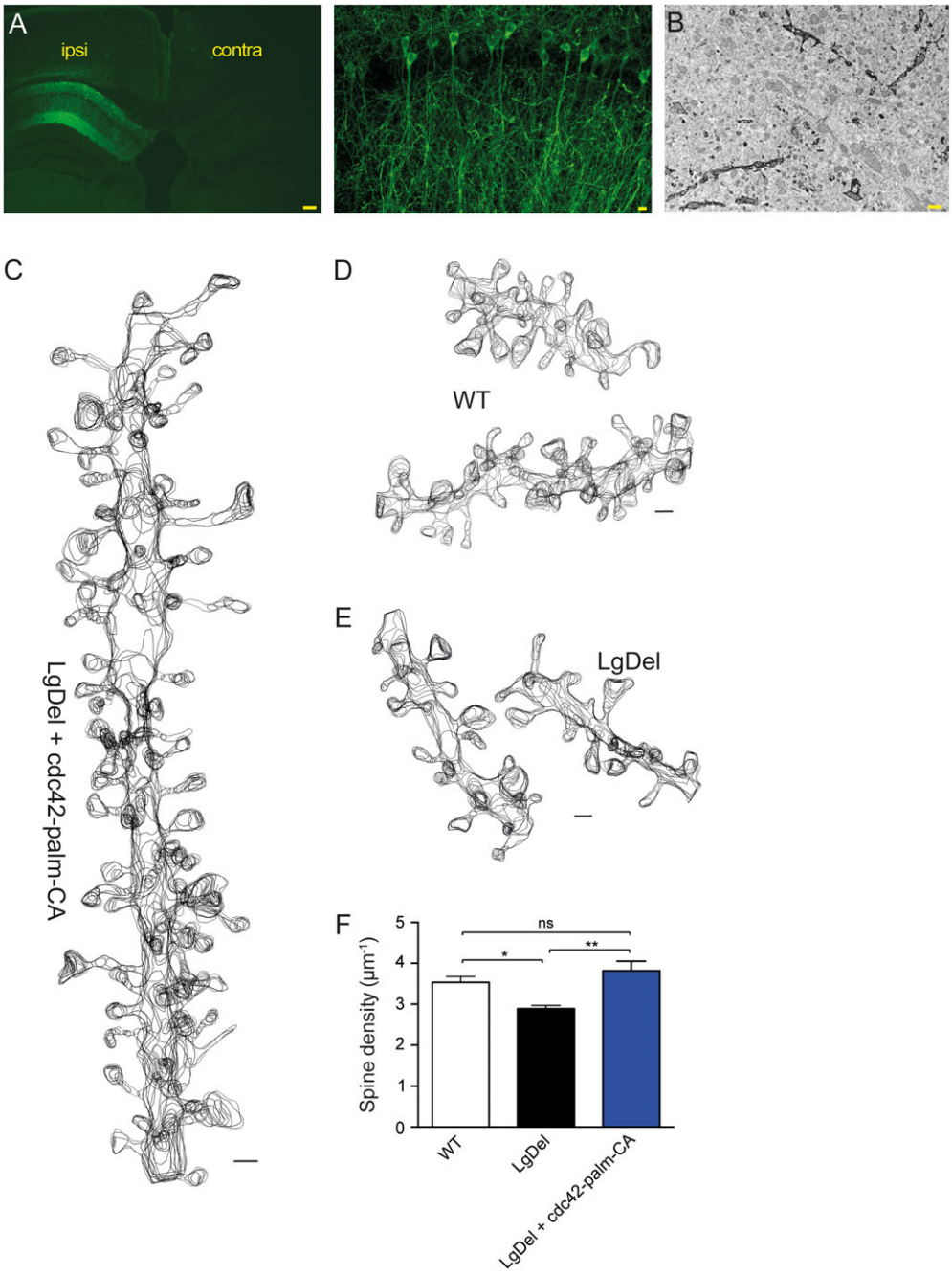

Figure 5. In vivo rescue of spine density in LgDel mice. (*A*) Representative images of coronal section of P37 LgDel mouse unilaterally injected at P7 in hippocampal CA1 area with AAV-Syn-eGFP-cdc42-palm-CA. Left, scale bar: 100 µm. Right: pyramidal neurons in the CA1 area expressing AAV-Syn- eGFP-cdc42-palm-CA. Scale bar: 10 µm. (*B*) EM image of the labeled dendritic segments from the CA1 neurons expressing AAV-Syn-eGFP-cdc42-palm-CA; Scale bar: 1 µm. (*C*) 3D reconstruction of the labeled dendritic segment from CA1 neuron in P41 LgDel mouse infected with AAV-Syn-eGFP-cdc42-palm-CA at P7. (*D*) 3D reconstruction of 2 dendritic segments in CA1 stratum radiatum neuropil of P41 WT mouse. (*E*) The same as *D* but in P41 LgDel mouse; in *C*, *D* and *E*: scale bars: 0.5 µm. (*F*) Spine density per unit length of dendrite in P41 WT, LgDel, and LgDel mice injected with AAV-Syn-eGFP-cdc42-palm-CA, quantified with EM. Data show the averages ± SEM of spine densities on 9 to 10 dendritic segments. *$P < 0.05$. **$P < 0.01$. ns: not significant; one-way ANOVA. Further details on the EM analysis in the Material and Methods section.

spine formation at the very starting point of spinogenesis, it shows, together with the increased spine turnover and unchanged spine formation/elimination 24 h-ratio, that LgDel mice brain, despite producing more spines than normal, has an alteration in the processes underlying long-term spine stabilization. This may explain the persistence of low spine density all along postnatal development, up to the adult age. Spine structural and/or functional impairment is a common feature of most psychiatric diseases (Penzes et al. 2011), and our study provides an insight on the role of long-term spine dynamics in synaptic networks formation and maintenance.

The Palmitoylation Deficit Behind the Spine Dynamics in LgDel Mice

During the last decade, palmitoylation has emerged as a critical regulator of structural and synaptic plasticity (El-Husseini et al. 2002; Fukata et al. 2004, 2013; Dejanovic et al. 2014). One of the

deleted genes in 22q11DS, *zdhhc8*, belongs to the family of PATs and was shown to be involved in spine density deficits in dissociated cultures of a mouse model of 22q11DS (Mukai et al. 2008), the observation also confirmed in our study. Using overexpression and knockdown approaches together with confocal repetitive imaging, we could further reveal the role of ZDHHC8 palmitoylation in spine stabilization. Importantly, ZDHHC8 expression in LgDel organotypic slices fully rescued spine density by increasing spine stability, without affecting spine formation.

Among the proteins that may fail to regulate spine stabilization in LgDel mice because of an impairment of palmitoylation, a strong body of arguments pointed at PSD-95. First, PSD-95 expression in neurons was shown to increase spine density (El-Husseini et al. 2000). Furthermore, PSD-95 is considered as a hub molecule involved in coupling fast synaptic responses with adhesion molecules (Han and Kim 2008) and its expression in nascent spines has been shown to correlate with spine survival in hippocampal organotypic cultures (De Roo et al. 2008a) as well as in mouse neocortical L2/3 pyramidal cells in vivo (Cane et al. 2014). Also, PSD-95 has been identified as a substrate of ZDHHC8 and suggested to underlie the spine density deficit in 22q11DS (Mukai et al. 2008). A recent palmitoylproteome study showed a 30% reduction of PSD-95 palmitoylation in cultured embryonic cortical neurons from *zdhhc8* knockout mice compared with WT mice (Mukai et al. 2015). However, we did not observe any modifications of PSD-95 palmitoylation in LgDel mice hippocampi. Redundancy among PATs for palmitoylation of PSD-95 has been indeed described and may explain this apparent discrepancy (Fukata et al. 2004). Although we cannot exclude the possibility that other PATs may show different levels of activity throughout life, in accordance with developmental needs, *ZDHHC8* expression was shown to be constant during development as demonstrated by temporal analysis of gene expression pattern of mouse orthologs of 22q11 genes (Maynard et al. 2003). Another explanation may be that in spite of haploinsufficiency of ZDHHC8 in LgDel mice, its activity might still remain sufficient to ensure full palmitoylation of PSD-95. Nevertheless, our data indicate that spine stabilization impairment observed in hippocampal organotypic cultures from LgDel mice is not due to a decreased palmitoylation of PSD-95.

The cdc42-Palmitoylation Impairment Behind the Spine Deficit in LgDel Mice

Another potentially interesting target of PATs is cdc42 from the Rho family of small GTPases. This protein is involved in actin cytoskeleton regulation and is necessary for spine stabilization (Vadodaria et al. 2013), correct spine density and long-term potentiation maintenance (Rex et al. 2009). Only the brain-specific splicing variant of cdc42, namely cdc42-palm can be palmitoylated, and this activity-dependent posttranslational modification seems to control spine density (Kang et al. 2008). We have found a drastic reduction of the palmitoylation level of cdc42-palm in LgDel hippocampi. This reduction was confirmed by Mukai et al. in a recent study in dissociated cortical neurons from *zdhhc8* knockout mice, although to a lesser extent (Mukai et al. 2015). This led us to study spine turnover and stabilization in LgDel mice during overexpression of a constitutively active form of cdc42-palm. In these conditions, we set back normal long-term spine stabilization in hippocampal organotypic cultures from LgDel mice. Interestingly, Mukai et al. also revealed an important role of cdc42-palm as a main relay of the effect of impaired palmitoylation on axonal growth, in line with previous studies that characterized the role of cdc42 in neuronal development (Scott et al. 2003; Chen et al. 2012). But importantly, our strategy consisted in overexpressing cdc42-palm-CA in a very low number of neurons and then studying the effect of this overexpression on the dendritic spines. This experimental design allowed to reveal a postsynaptic action of cdc42-palm-CA and to identify the role of cdc42 palmitoylation in the long-term spine stabilization impairment in a genetic mouse model of 22q11DS. These results are of particular importance in the context of synaptic and structural plasticity. First, spine stabilization is selectively increased in spines that are activated by learning-related patterns of plasticity (De Roo et al. 2008b) and second, cdc42 activation rapidly relays CaM kinase II activation to translate synaptic plasticity into morphological changes in spines following their activation by 2-photon glutamate uncaging (Kim et al. 2014).

In a more general context and together with Mukai data (Mukai et al. 2015), our study indicates that under the control of ZDHHC8, the brain variant of cdc42 may exert different presynaptic and postsynaptic roles in wiring formation and network adaptation depending on the developmental stage of the brain. This is of particular importance in the field of psychiatric disease of genetic origin, such as 22q11DS, where therapeutic attempts may be done at specific early stages, when neuronal networks are still very plastic (Takesian and Hensch 2013). In this line, our strategy consisting of injecting a vector containing cdc42-palm-CA at a very young age proved successful as it resulted in a full rescue of spine density in adult mice. Specific behavioral tests may provide more information about the consequences of this rescue at the cognitive level.

The Pathophysiological Significance of an Altered Long-term Spine Stability in the Context of 22q11DS and Schizophrenia

Children affected by 22q11DS show mild cognitive deficit and have 30% probability to become schizophrenic or express schizotypic behavior (Pulver et al. 1994). Neurophysiological models of schizophrenia suggest that disruptions in higher order cognitive and emotional functions are driven by impairments in elementary perceptual processes (Javitt 2009). In this study, in a genetic model of 22q11DS, we identified impairment in a very basic feature of structural plasticity, which is the inability of a neuron to maintain its synapses in the long term. As long-term spine stabilization is closely related to structural and synaptic plasticity (Caroni et al. 2012), this impairment is likely to prevent local and distant neuronal circuits from assembling together in an appropriate manner. Furthermore, this impairment in spine stabilization is accompanied by an increase in spine formation, which might be a compensating mechanism of LgDel neurons to maintain spine density at a normal level. This excessive formation of new spines may promote the creation of aberrant neuronal circuits. This is in agreement with the dysconnection hypothesis in schizophrenia, which has been proposed to originate from an aberrant synaptic wiring during development (McGlashan and Hoffman 2000). This hypothesis is also specifically explored in 22q11DS patients (Ottet et al. 2013). To date, the principal mechanism thought to underlie this dysconnectivity is a dysregulation of neuromodulatory inputs on N-methyl-D-aspartate receptor-mediated pathways, leading to an aberrant synaptic plasticity (Stephan et al. 2009).

Our results provide an additional structural mechanism to the dysconnection hypothesis, translated as an impairment

of spine stabilization. By identifying 2 of its molecular determinants, ZDHHC8 and cdc42-palm, we provide leads for future therapeutic treatments of 22q11DS based on drugs targeting these proteins. This is particularly relevant as, given their important and various roles in pathophysiology, pharmacological approaches to modulate palmitoylation and cdc42 are already at the focus of research in drug design (Chavda et al. 2014).

Overall, this work highlights the role of ZDHHC8-cdc42-palm pathway in the physiological control of postsynaptic structural plasticity. As palmitoylation is reversible and tightly regulated by the activity (Kang et al. 2008; Noritake et al. 2009; Fukata et al. 2013), we propose that this dynamic posttranslational process could be one of the important plasticity control mechanisms that is affected in 22q11DS, a schizophrenia-related pathology.

Supplementary Material

Supplementary material can be found at: http://www.cercor.oxfordjournals.org/.

Funding

The People Programme (Marie Curie Actions) of the European Union's Seventh Framework Programme FP7/2007-2013 (grant 289581); The Swiss National Science Foundation (grant 310030B-144080) to D.M.; The National Center of Competence in Research Synapsy (D.M.); and the German Research council (DFG, grant Po732) to E.P.

Notes

This paper is dedicated to the memory of Dominique Muller, whose ideas about structural and synaptic plasticity inspired this study and will continue to inspire all of us (Dominique passed away 29 April 2015).

The authors wish to address their heartiest thanks to Lorena Jourdain for her technical help and support. We acknowledge the iGE3 genomics platform of the university of Geneva (http://www.ige3.unige.ch/genomics-platform.php) and especially Didier Cholet who performed RT-PCRs. We also gratefully acknowledge Raju Kucherlapati (Harvard Medical School, Boston) for the generous gift of the LgDel mouse model. We are grateful to Martin Werno and Luke Chamberlain for experimental help and advice. *Conflict of Interest:* None declared.

References

Arguello PA, Gogos JA. 2010. Cognition in mouse models of schizophrenia susceptibility genes. Schizophr Bull. 36:289–300.

Bhatt DH, Zhang S, Gan WB. 2009. Dendritic spine dynamics. Annu Rev Physiol. 71:261–282.

Cane M, Maco B, Knott G, Holtmaat A. 2014. The relationship between PSD-95 clustering and spine stability in vivo. J Neurosci. 34:2075–2086.

Carlson C, Sirotkin H, Pandita R, Goldberg R, McKie J, Wadey R et al. 1997. Molecular definition of 22q11 deletions in 151 velo-cardio-facial syndrome patients. Am J Hum Genet. 61:620–629.

Caroni P, Donato F, Muller D. 2012. Structural plasticity upon learning: regulation and functions. Nat Rev Neurosci. 13:478–490.

Chavda B, Arnott JA, Planey SL. 2014. Targeting protein palmitoylation: selective inhibitors and implications in disease. Expert Opin Drug Discov. 9:1005–1019.

Chen C, Wirth A, Ponimaskin E. 2012. Cdc42: an important regulator of neuronal morphology. Int J Biochem Cell Biol. 44:447–451.

De Roo M, Klauser P, Mendez P, Poglia L, Muller D. 2008a. Activity-dependent PSD formation and stabilization of newly formed spines in hippocampal slice cultures. Cereb Cortex. 18:151–161.

De Roo M, Klauser P, Muller D. 2008b. LTP promotes a selective long-term stabilization and clustering of dendritic spines. PLoS Biol. 6:e219.

Dejanovic B, Semtner M, Ebert S, Lamkemeyer T, Neuser F, Luscher B et al. 2014. Palmitoylation of gephyrin controls receptor clustering and plasticity of GABAergic synapses. PLoS Biol. 12:e1001908.

El-Husseini AE, Schnell E, Chetkovich DM, Nicoll RA, Bredt DS. 2000. PSD-95 involvement in maturation of excitatory synapses. Science. 290:1364–1368.

El-Husseini A-D, Schnell E, Dakoji S, Sweeney N, Zhou Q, Prange O et al. 2002. Synaptic strength regulated by palmitate cycling on PSD-95. Cell. 108:849–863.

Engert F, Bonhoeffer T. 1999. Dendritic spine changes associated with hippocampal long-term synaptic plasticity. Nature. 399:66–70.

Fenelon K, Mukai J, Xu B, Hsu PK, Drew LJ, Karayiorgou M et al. 2011. Deficiency of Dgcr8, a gene disrupted by the 22q11.2 microdeletion, results in altered short-term plasticity in the prefrontal cortex. Proc Natl Acad Sci U S A. 108:4447–4452.

Fenelon K, Xu B, Lai CS, Mukai J, Markx S, Stark KL et al. 2013. The pattern of cortical dysfunction in a mouse model of a schizophrenia-related microdeletion. J Neurosci. 33:14825–14839.

Forrester MT, Hess DT, Thompson JW, Hultman R, Moseley MA, Stamler JS et al. 2011. Site-specific analysis of protein S-acylation by resin-assisted capture. J Lipid Res. 52:393–398.

Fukata Y, Dimitrov A, Boncompain G, Vielemeyer O, Perez F, Fukata M. 2013. Local palmitoylation cycles define activity-regulated postsynaptic subdomains. J Cell Biol. 202:145–161.

Fukata Y, Fukata M. 2010. Protein palmitoylation in neuronal development and synaptic plasticity. Nat Rev Neurosci. 11:161–175.

Fukata M, Fukata Y, Adesnik H, Nicoll RA, Bredt DS. 2004. Identification of PSD-95 palmitoylating enzymes. Neuron. 44:987–996.

Goldberg R, Motzkin B, Marion R, Scambler PJ, Shprintzen RJ. 1993. Velo-cardio-facial syndrome: a review of 120 patients. Am J Med Genet. 45:313–319.

Han K, Kim E. 2008. Synaptic adhesion molecules and PSD-95. Prog Neurobiol. 84:263–283.

Holtmaat A, Svoboda K. 2009. Experience-dependent structural synaptic plasticity in the mammalian brain. Nat Rev Neurosci. 10:647–658.

Holtmaat AJ, Trachtenberg JT, Wilbrecht L, Shepherd GM, Zhang X, Knott GW et al. 2005. Transient and persistent dendritic spines in the neocortex in vivo. Neuron. 45:279–291.

Javitt DC. 2009. When doors of perception close: bottom-up models of disrupted cognition in schizophrenia. Annu Rev Clin Psychol. 5:249–275.

Kang R, Wan J, Arstikaitis P, Takahashi H, Huang K, Bailey AO et al. 2008. Neural palmitoyl-proteomics reveals dynamic synaptic palmitoylation. Nature. 456:904–909.

Karayiorgou M, Simon TJ, Gogos JA. 2010. 22q11.2 microdeletions: linking DNA structural variation to brain dysfunction and schizophrenia. Nat Rev Neurosci. 11:402–416.

Kasai H, Fukuda M, Watanabe S, Hayashi-Takagi A, Noguchi J. 2010. Structural dynamics of dendritic spines in memory and cognition. Trends Neurosci. 33:121–129.

Kim IH, Wang H, Soderling SH, Yasuda R. 2014. Loss of Cdc42 leads to defects in synaptic plasticity and remote memory recall, Elife. 1–16. doi: 10.7554/eLife.02839.

Lin DT, Makino Y, Sharma K, Hayashi T, Neve R, Takamiya K et al. 2009. Regulation of AMPA receptor extrasynaptic insertion by 4.1N, phosphorylation and palmitoylation. Nat Neurosci. 12:879–887.

Long JM, LaPorte P, Merscher S, Funke B, Saint-Jore B, Puech A et al. 2006. Behavior of mice with mutations in the conserved region deleted in velocardiofacial/DiGeorge syndrome. Neurogenetics. 7:247–257.

Maynard TM, Haskell GT, Peters AZ, Sikich L, Lieberman JA, LaMantia AS. 2003. A comprehensive analysis of 22q11 gene expression in the developing and adult brain. Proc Natl Acad Sci U S A. 100:14433–14438.

McGlashan TH, Hoffman RE. 2000. Schizophrenia as a disorder of developmentally reduced synaptic connectivity. Arch Gen Psychiatry. 57:637–648.

Meechan DW, Rutz HL, Fralish MS, Maynard TM, Rothblat LA, LaMantia AS. 2015. Cognitive ability is associated with altered medial frontal cortical circuits in the LgDel mouse model of 22q11.2DS. Cereb Cortex. 25:1143–1151.

Merscher S, Funke B, Epstein JA, Heyer J, Puech A, Lu MM et al. 2001. TBX1 is responsible for cardiovascular defects in velo-cardio-facial/DiGeorge syndrome. Cell. 104:619–629.

Meyer D, Bonhoeffer T, Scheuss V. 2014. Balance and stability of synaptic structures during synaptic plasticity. Neuron. 82:430–443.

Milnerwood AJ, Parsons MP, Young FB, Singaraja RR, Franciosi S, Volta M et al. 2013. Memory and synaptic deficits in Hip14/DHHC17 knockout mice. Proc Natl Acad Sci U S A. 110:20296–20301.

Moutin E, Raynaud F, Fagni L, Perroy J. 2012. GKAP-DLC2 interaction organizes the postsynaptic scaffold complex to enhance synaptic NMDA receptor activity. J Cell Sci. 125: 2030–2040.

Mukai J, Dhilla A, Drew LJ, Stark KL, Cao L, MacDermott AB et al. 2008. Palmitoylation-dependent neurodevelopmental deficits in a mouse model of 22q11 microdeletion. Nat Neurosci. 11:1302–1310.

Mukai J, Tamura M, Fenelon K, Rosen AM, Spellman TJ, Kang R et al. 2015. Molecular substrates of altered axonal growth and brain connectivity in a mouse model of schizophrenia. Neuron. 86:680–695.

Nikonenko I, Boda B, Steen S, Knott G, Welker E, Muller D. 2008. PSD-95 promotes synaptogenesis and multiinnervated spine formation through nitric oxide signaling. J Cell Biol. 183: 1115–1127.

Nikonenko I, Nikonenko A, Mendez P, Michurina TV, Enikolopov G, Muller D. 2013. Nitric oxide mediates local activity-dependent excitatory synapse development. Proc Natl Acad Sci U S A. 110:E4142–51.

Noritake J, Fukata Y, Iwanaga T, Hosomi N, Tsutsumi R, Matsuda N et al. 2009. Mobile DHHC palmitoylating enzyme mediates activity-sensitive synaptic targeting of PSD-95. J Cell Biol. 186:147–160.

Ottet MC, Schaer M, Debbane M, Cammoun L, Thiran JP, Eliez S. 2013. Graph theory reveals dysconnected hubs in 22q11DS and altered nodal efficiency in patients with hallucinations. Front Hum Neurosci. 7:402.

Paylor R, McIlwain KL, McAninch R, Nellis A, Yuva-Paylor LA, Baldini A et al. 2001. Mice deleted for the DiGeorge/velocardiofacial syndrome region show abnormal sensorimotor gating and learning and memory impairments. Hum Mol Genet. 10:2645–2650.

Penzes P, Cahill ME, Jones KA, VanLeeuwen JE, Woolfrey KM. 2011. Dendritic spine pathology in neuropsychiatric disorders. Nat Neurosci. 14:285–293.

Pulver AE, Nestadt G, Goldberg R, Shprintzen RJ, Lamacz M, Wolyniec PS et al. 1994. Psychotic illness in patients diagnosed with velo-cardio-facial syndrome and their relatives. J Nerv Ment Dis. 182:476–478.

Rex CS, Chen LY, Sharma A, Liu J, Babayan AH, Gall CM et al. 2009. Different Rho GTPase-dependent signaling pathways initiate sequential steps in the consolidation of long-term potentiation. J Cell Biol. 186:85–97.

Salaun C, Greaves J, Chamberlain LH. 2010. The intracellular dynamic of protein palmitoylation. J Cell Biol. 191:1229–1238.

Scott EK, Reuter JE, Luo L. 2003. Small GTPase Cdc42 is required for multiple aspects of dendritic morphogenesis. J Neurosci. 23:3118–3123.

Shprintzen RJ, Goldberg RB, Lewin ML, Sidoti EJ, Berkman MD, Argamaso RV et al. 1978. A new syndrome involving cleft palate, cardiac anomalies, typical facies, and learning disabilities: velo-cardio-facial syndrome. Cleft Palate J. 15:56–62.

Stark KL, Xu B, Bagchi A, Lai WS, Liu H, Hsu R et al. 2008. Altered brain microRNA biogenesis contributes to phenotypic deficits in a 22q11-deletion mouse model. Nat Genet. 40:751–760.

Stephan KE, Friston KJ, Frith CD. 2009. Dysconnection in schizophrenia: from abnormal synaptic plasticity to failures of self-monitoring. Schizophr Bull. 35:509–527.

Sterio DC. 1984. The unbiased estimation of number and sizes of arbitrary particles using the disector. J Microsc. 134:127–136.

Stoppini L, Buchs PA, Muller D. 1991. A simple method for organotypic cultures of nervous tissue. J Neurosci Methods. 37:173–182.

Takesian AE, Hensch TK. 2013. Balancing plasticity/stability across brain development. Prog Brain Res. 207:3–34.

Thomas GM, Hayashi T, Huganir RL, Linden DJ. 2013. DHHC8-dependent PICK1 palmitoylation is required for induction of cerebellar long-term synaptic depression. J Neurosci. 33:15401–15407.

Vadodaria KC, Brakebusch C, Suter U, Jessberger S. 2013. Stage-specific functions of the small Rho GTPases Cdc42 and Rac1 for adult hippocampal neurogenesis. J Neurosci. 33: 1179–1189.

Wirth A, Chen-Wacker C, Wu YW, Gorinski N, Filippov MA, Pandey G et al. 2013. Dual lipidation of the brain-specific Cdc42 isoform regulates its functional properties. Biochem J. 456:311–322.

Xu B, Hsu PK, Stark KL, Karayiorgou M, Gogos JA. 2013. Derepression of a neuronal inhibitor due to miRNA dysregulation in a schizophrenia-related microdeletion. Cell. 152: 262–275.

Yoshihara Y, De Roo M, Muller D. 2009. Dendritic spine formation and stabilization. Curr Opin Neurobiol. 19:146–153.